Optimization of Operating Parameters Using Response Surface Methodology for Preparation of Sugarcane Bagasse-Derived Activated Carbon Via Chemical Activation

Waranya Vitooniput* Dr.Varinrumpai Seithtanabutara[1]**

(Received: *March 1, 2019*; Revised: *April 12, 2019*; Accepted: *April 18, 2019*)

ABSTRACT

The sugarcane bagasse-derived activated carbon was synthesized via impregnation-carbonization method. The different weight ratio of $ZnCl_2$ (1:1 to 1:3), carbonization temperature and time of 400-600°C and 60 to 120 min respectively were designed using Box-Behnken Design Minitab. The porous, textural, structural and thermal stability of produced activated carbon will be characterized by N_2 adsorption/desorption, SEM, FTIR respectively. SCB-AC of 1298 m^2/g was produced at optimum condition; $ZnCl_2$ concentration, carbonization temperature and time of 2.19 M, 488.89°C and 95.18 min respectively. The produced AC had an irregular structure consisting of both micropores and mesopores, different functional groups and high thermal stability. The SCB-AC with the highest specific surface area of 1355.7 m^2/g can be further applied for the next relevant works.

Keywords: Activated carbon, Zinc Chloride, Box-behnken

[1]*Correspondent author: tmaillka@kku.ac.th*

**Student, Master of Engineering Program in Energy Engineering, Faculty of Engineering, Khon Kaen University*

***Assistant Professor, Department of Chemical Engineering, Faculty of Engineering, Khon Kaen University*

Introduction

Activated carbons (Acs) have been widely used in various applications such as separation and purification of gaseous and liquid mixtures, fuel storage, air purification, groundwater remediation etc. Carbonization and activation process are involved in the preparation of activated carbons. Physical activation can be done in the presence of high oxidizing agent such as steam, CO_2, O_2 or a mixture of them. Differently from chemical activation, the starting material is impregnated with a chemical agent followed by carbonization in an inert atmosphere. The benefits of chemical activation over physical activation are simplicity, simultaneous carbonization-activation, higher global yield based on starting material weight, shorter activation time, lower carbonization temperature, less energy consumption and greater porous structure development [1]. Activating agents; alkalis and alkaline earth metals and other acid salts such as $ZnCl_2$, $MgCl_2$, NaOH, K_2CO_3 and KOH have been reported for the chemical activation method [2]. Among various agents, $ZnCl_2$ is one of the promising transition metal salt widely used in the preparation of activated carbon. The $ZnCl_2$ activation has an ability from its dehydrating function to create porosity in carbon precursors. The enhancement of porosity generation and carbon content via $ZnCl_2$ activation are resulted from the elimination of hydrogen and oxygen atoms in water form rather than oxygenated compounds of carbon material [3]. Many investigations have been presented the AC production from biomass waste; coconut husk, nutshell, wood, corncob, rubber seed shell and agricultural products and wastes [1-4]. Sugarcane bagasse (SCB) is one of interesting precursor for activated carbon production due to its high density, high carbon contents and low ash, availability in large quantities at low costs [5]. Microporous activated carbon derived from SCB with high surface area of 661.46 m^2/g was obtained at the carbonization temperature of 800°C by physical activation with CO_2 gas for 120 min [6]. Base-leaching pretreatment of SCB enhanced the surface area and pore structure of produced activated carbon. Zinc chloride activation gave the activated carbon with larger surface area and pore volume than that from phosphoric acid activation [7]. However, its pore development and surface characteristics depended on precursor type, activating agent, the concentration of chemical agent, activation time, carbonization temperature and carbonization time. Currently, a few report on optimization of the production of activated carbon with high surface area using the response surface methodology (RSM) approach [8-10]. RSM was applied to find the most optimum conditions from several numbers of experiments as well as reduction in experimental time, saving both material and personnel cost. Box-Behnken Designs (BBD) is considered as an efficient option in RSM and owing to have fewer design points, less expensive, more saving time and have opportunities to optimize more parameters than in Central Composite Design (CCD) [9]. In this study, RSM based on BBD was applied to optimize the production of high surface area activated carbon from SCB using zinc chloride as the activating agent. Design factors were the impregnated chemical concentration, carbonization temperature and time with three varying level settings. The optimum conditions for SCB-AC production were evaluated. The porous, textural, structural and physical properties of produced activated carbon will be characterized and discussed.

Methodology

Sugar cane bagasse (SCB) was-collected from sugar industry in northeastern region of Thailand. Analytical grade chemicals, NaOH, $ZnCl_2$, HCl were used. SCB was milled prior to be pretreated by NaOH of 0.5 M at 80°C under continuous magnetic stirring for 1 hour. Then it was dried at 100°C for 3 hours before $ZnCl_2$ impregnation for 24 hours. The ratio of SCB to $ZnCl_2$ solution of 1-3 M was kept constant at 40 g/300 ml. The SCB was separated and dried in an oven at 100°C for 6 hours before carbonization in electric furnace under nitrogen atmosphere with the flowrate of 3 cm^3/min at 500-700°C for 60-120 min. The SCB-AC was washed with hot distilled water until neutral and was dried in oven at 100°C for 1 hour. The Box–Behnken design (BBD) of RSM method was applied for the experimental design using Minitab 16 statistical software. To investigate the effects of operating parameters on the specific surface area (Y, m^2/g) of produced activated carbon, three operating factors were chosen; $ZnCl_2$ concentration (A, molar), carbonization temperature (B, °C) and carbonization time (C, min). The experimental range of these factors were 1-3 M, 500-700°C and 60-120 min respectively. A 3-factor–3-level BBD with a total of 15 trials were performed as shown in Table 1, all response value for each run was recorded as the mean of triplicates. To correlate the dependent and independent variables, the experimental data was analyzed by the response surface regression procedure to fit the following second-order polynomial response equation (1).

$$Y=\beta_0 + \beta_1 A + \beta_2 B + \beta_3 C + \beta_{12} AB + \beta_{13} AC + \beta_{23} BC + \beta_{11} A^2 + \beta_{22} B^2 + \beta_{33} C^2 \quad (1)$$

Where Y is the response; β_0 is constant; β_1, $\beta_2$and β_3 are the linear coefficients; β_{12}, β_{13} and β_{23} are cross product coefficients; β_{11}, β_{22} and β_{33} are the squared coefficient. The reduced model was achieved using ANOVA for the statistical significance of the main effects, interactions, coefficients and residues error. The quality of the fit of the regression model was expressed with the coefficient of determinations (R^2,R_{adj}^2) and statistical significance was checked by the F-test. Model terms were selected or rejected based on the probability value with 95% confident level. The 3D response surfaces and contour plots were drawn to visualize the individual and interactive effects of the independent variables on the specific surface area of obtained activated carbon. The optimum condition of operating variables was obtained and three replicated runs were performed in order to check the validity of the predicted model. The mean response values were obtained as shown in Table 1.

The structured-porous characteristics were investigated by N_2 adsorption/desorption at 196°C in the range of relative pressure 0.001-0.3 bar. using Micromeritics ASAP 2010. The BET specific surface area (S_{BET}) of AC was calculated using Branauer- Emmet and Teller (BET) equation. The micropore surface area (S_{mi}) was calculated by applying t-plot micropore area. The mesopore surface area (S_{me}) was obtained from the subtraction S_{mi} from S_{BET}. The total pore volume (V_T) was estimated from the amount of N_2 adsorbed at relative high pressure (P/P_0 ~0.99). The micropore volume (V_{mi}) was obtained from t-plot micropore volume. The mesopore volume (V_{me}) was calculated by subtracting V_{mi} from V_T. The BJH (Barrett-Joyner-Halenda) model was used to determine the pore size distribution of AC samples. Scanning Electron Microscope (SEM S-3000N, HITACHI) operating at magnification of 800-2000 was used for the surface morphology of raw SCB and products. The functional groups of samples were examined using the Fourier Transform Infrared Spectroscopy (FTIR, S5_iD5, Thermo Scientific Nicolet) recording the IR spectrum in the

range of 600-4000 1/cm. Thermogravimetric analyzer (TGA, 50-Shimadzu Japan) was used to analyze the properties and thermal stabilities under nitrogen atmosphere with heating rate of 10°C/min under N_2 atmosphere from room temperature to 700°C. The percentage of weight loss of sample was observed in the function of the heating time and temperature.

Table 1 The variation of factors, level setting and responses for each experiment

RUN	B (°C)	C (min)	Y (specific surface area, m^2/g)	
			Experimental	**Predicted value**
1	400	90	772.12	671.384
2	500	60	507.83	592.156
3	600	120	976.23	877.903
4	500	90	1355.71	1291.337
5	400	120	821.01	976.115
6	500	60	866.37	838.821
7	400	90	867.12	918.049
8	500	120	636.87	728.129
9	400	60	945.44	840.143
10	500	120	1122.83	974.794
11	500	90	1,229.76	1,291.337
12	600	90	648.02	573.171
13	600	90	695.18	819.836
14	600	60	693.41	741.93
15	500	90	1,288.54	1,291.337

Results and Discussion

The significant evaluation from the relation among three operating factors; concentration of the activating agent, carbonizing temperature and time, was conducted in order to investigate the optimum condition on production of activated carbon having the high specific surface. It was found that the highest mean response of the specific surface area was presented at using $ZnCl_2$ concentration of 2 M, carbonization at 500°C and carbonization time for 90 min. The relationship between the response (Y) and the independent variables in the coded units (A, B and C) in the form of empirical full quadratic equation for predicting the optimum condition was achieved through the Box–Behnken design. The significance of the coefficient term was proved by the values of P and F. The residual error corresponding to each coefficients as well as the relation between pure error and lack-of-fit which accounted to determine the failure of a model were used to approximate the F value. The F-value was estimated using the experimental data corresponded to the total residual. The proposed model was significant in the region studied if the F-value estimated using the experimental data corresponded to the total residual was greater than the tabular F-value distribution for a certain number of degrees of freedom in the model at the level of significance α. The ''Lack-of-Fit F-value'' also measures the failure of a model to represent the data in the experimental sphere at points which are not included in the regression. The lack-of-fit is statistically insignificance to the pure error if F-value estimated using the experimental data corresponded to the lack-of-fit was less than tabular F-value. Table 2 shows the ANOVA results of adjusted model

after elimination of insignificant terms (P>0.05) of full quadratic equation. The acceptability of model fit was confirmed in which F-value of this model (8.32) is obviously greater than the tabular F-value (3.58) indicated the variable was significant to the residual error. Also, its F value corresponding to the lack of fit with the pure error (5) was less than tabular F-value (19.33) revealing that the lack of fit is not significant relative to the pure errors. On investigating the coefficient of determination (R^2) value of 0.8617 was in reasonable agreement with the ''Adjusted R^2'' of 0.7584. Thus, all these statistical tests showed that quadratic models developed proved to be successful in good predictability and fitting between the process variables and responses.

$$Y = -7808.57 + 1365.88X_1 + 23.02X_2 + 41.71X_3 + -310.64{X_1}^2 - 0.02{X_2}^2 - 0.22{X_3}^2 \quad (2)$$

Table 2 Analysis of variance for BET (m^2/g)

Source	DF	Seq SS	Adj SS	Adj MS	F	P
Regression	6	793402	793402	132234	8.32	0.004
Linear	3	177956	677826	225942	14.22	0.001
A	1	121687	418459	418459	26.34	0.001
B	1	19291	194728	194728	12.26	0.008
C	1	36977	158566	158566	9.98	0.013
Square	3	615446	615446	205149	12.91	0.002
A^2	1	292187	356291	356291	22.42	0.001
B^2	1	179638	204063	204063	12.84	0.007
C^2	1	143622	143622	143622	9.04	0.017
Residual Error	8	127107	127107	15888		
Lack-of-Fit	6	119163	119163	19861	5	0.176
Pure Error	2	7943	7943	3972		
Total	14	920509				
R^2 = 86.19%, R^2_{adj} = 75.84%						

The 3D response surfaces and contour plots holding one parameter as a constant at the medium level as shown in Figure 1 were obtained in order to consider the effects of each variable and its mutual interaction on the response. The surface effect plot and the contour in the relation between carbonization time (C) and carbonization temperature (B) with holding the $ZnCl_2$ concentration at a constant value of 2 M were presented the Figure 1(a) and Figure 1(d), respectively. The response increased gradually upon increasing in carbonization temperature and time. It can be observed that the maximum response was set between 460.46 - 517.35°C and 85.60 - 104.40 min. Considering the interaction between the $ZnCl_2$ concentration (A) and carbonization time (C) by keeping the carbonization temperature as constant value at 500°C was shown in Figure 1(b) and Figure 1(e). It was found that the response was increased due to the increasing in $ZnCl_2$ concentration and carbonization time to 1.60 M and 72.79 min, then it slowly decreased along the increasing of $ZnCl_2$ and carbonization time from 2.78, 117.19 respectively. The 3D response surface an contour plot corresponding to the $ZnCl_2$ concentration (A) and carbonization temperature (B) while the carbonization time was constantly held at 90 min was shown in Figure 1(c) and Figure 1(f), respectively. The response increased with the increasing of $ZnCl_2$ concentration and carbonization temperature starting from the 1.62 - 2.78 M and 424.08 - 557.38°C, respectively. Then the response value was shrinking down along the increasing in carbonization temperature

and concentration. The contour plot also described that the maximum range of specific surface area expressed at this range. Therefore, the $ZnCl_2$ concentration has the most effect to the response compared to the carbonization temperature and time.

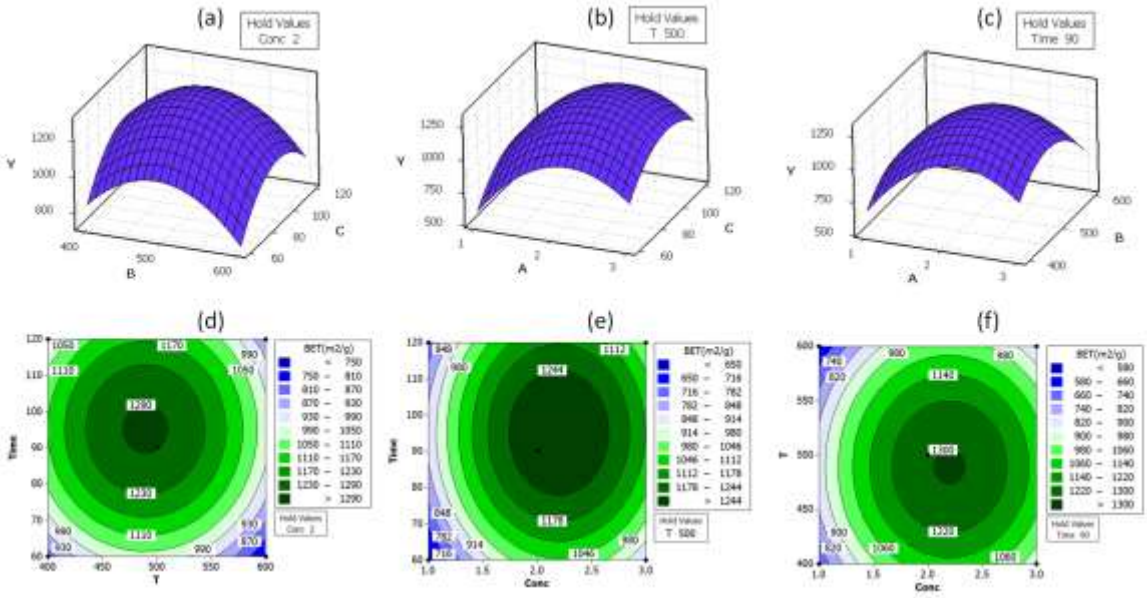

Figure 1 3D response surfaces and contour plots showing the effects of variable (A: $ZnCl_2$ concentration (M), B : carbonization temperature (°C) and C: carbonization time (min)) on the specific surface area of ACs.

Table 3 The pore structure assessment of all selected samples

	Char	S2	Sopt	S4
Condition: $ZnCl_2$ concentration (M)	0	3.00	2.19	2.00
Activating temperature (°C)	488.8	600.0	488.8	500.00
Activating time (min)	95.18	90.00	95.18	90.00
Porous properties : BET (m^2/g)	262.0	508.7	1298.	1355.70
Average pore Diameter (A^0)	2.38	2.24	2.07	2.04
S_{Micro} (m^2/g)	113.8	183.9	352.2	448.95
S_{Meso} (m^2/g)	148.2	324.8	945.7	906.75
$V_{Total\ Pore}$ (cm^3/g)	0.16	0.29	0.58	0.58
V_{Micro} (cm^3/g)	0.06	0.09	0.16	0.22
V_{Meso} (cm^3/g)	0.10	0.20	0.42	0.36
S_{micro}/S_{BET} (%)	43.42	36.15	27.14	33.12
S_{meso}/S_{BET} (%)	56.58	63.85	72.86	66.88
V_{Micro}/ V_{total} (%)	37.50	31.03	28.23	38.40
V_{Meso}/ V_{total} (%)	62.50	68.97	71.77	61.60

The response optimizer in MINITAB (version 16) software was used to determine the condition for production of the activated carbon with maximum response. The experimental conditions with the highest composite desirability

were selected to be verified. The optimal condition for production of SCB derived-ACs with high specific surface area of 1,312 m^2/g was using $ZnCl_2$ concentration of 2.19 M in SCB impregnation step before carbonization at 488.89°C for 95.18 min. To check validity and reliability of predicted model, the replicated experimental three runs at this condition were conducted. The average experimental value (1,298 m^2/g) was closed to the predicted value (1,312 m^2/g) with relatively small errors of 0.48. Therefore, the RSM was effective and reliable for optimizing the production condition of SCB derived-activated carbon with high specific surface area. SCB-char and selected SCB-ACs (S2, Sopt and S4) were investigated for pore structure analysis including pore structure assessment, N_2 adsorption/desorption isotherms and pore size distribution properties. The SCB-char was prepared at the optimum condition; 488.89°C and 95.18 min without $ZnCl_2$ impregnation. While S2 and S4 had the minimum and maximum specific surface area respectively . Table 3 shows the specific surface area, pore structure and pore volume of these selected samples, the SCB-char had the biggest average pore diameter of 2.38 Å with specific surface area of 262.07 m^2/g. Tzong-Horng Liou [7]. has reported that base-leaching of raw material can obviously affect to the adsorption capacity of carbon due to its ash eliminating property by forming sodium silicate (Na_2SiO_3) solution from the reaction between silica and NaOH. When the sodium silicate was removed by the filtration, the pores were increased compared to the carbon precursor without any base treatment. NaOH can also softened the material with organic tissue resulting in higher interior contacting surface of the activating agent during the impregnation process which can promote in pore development. The increase in miscelle voids including both inter and intra void was caused by lateral bonds cracking from the swelling effect by electrolytic action which occurred in cellulose molecular structure. Eventually, the voids increasing can enhance the larger BET specific surface area [11]. It was concluded that zinc chloride plays an important role during the thermal degradation of the impregnated particle up to 500˚C. S2 showed the minimum specific surface area since $ZnCl_2$ had unreacted with char above the temperature higher than 500˚C, S4 with maximum specific surface area was produced at the condition of $ZnCl_2$ concentration of 2 M, the activating temperature of 500 ˚C and activating time of 90 min. This finding corresponded to the previous study of Tzong-Horng Liou [7] in which activated carbon with the highest specific surface area was produced via $ZnCl_2$ impreganation followed by carbonization at 500˚C because of the tar formation was completely released from the char surface . As the carbonization temperature increased, volatile matter had been huge evolved and the small pores were disrupted resulting in the decrease in specific surface area [7].

Therefore, alkaline pretreatment of precursor with using impregnation ratio of 2/1 ($ZnCl_2$: bagasse) had been effectively developed the micropore in AC structure [12]. The present study found that both factors had the vital role in increasing of volumetric percentage of micropore resulted in large specific surface area, as seen in S4. However, the structured porous surface of obtained activated carbons was mainly mesopores consistent to the previous work [13]. The interaction between solutes and adsorbent was pronounced by adsorption/desorption isotherm [14]. Figure 2(a) displays the relationship between adsorbed nitrogen volume and relative pressure of all selected derived AC and its char. According to the IUPAC classification, the adsorption/desorption isotherm of SCB-char and S were Type 1 indicating major structured-micropores. Isotherms of S2 and Sopt were the combination of type I and II denoted the

mesoporosity occurrence which is similar to that discussed in previous work of Hu et al. [12] that the development in mesoporous structure was occurred at the impregnation ratio of $ZnCl_2$ exceeds 2. It is obviously seen that the derived-AC with high specific surface area, S4 had better adsorption of nitrogen at any specific relative pressure acting as Type I isotherm of conventional activated carbon [12]. However, less porous structure of SCB-char without salt impregnation was confirmed by its isotherm as the lowest nitrogen had been absorped at relative pressure. These isotherms consistent with their specific surface area which indicated that N_2 adsorption/desorption capacity of AC depended on its specific surface area. The relation between pore size distribution and AC pore width of selected samples was obtained in Figure 2(b), based on BJH(Barrett-Joyner-Halenda) method. Commonly, the porous structure of activated carbon are classified as micropores, mesopores and macropores. The pore size of micropores, mesopores and macropores are defined as 2 nm diameter or smaller, 2–50 nm diameter and larger than 50 nm respectively. The pore size distribution (PSD) of derived-AC after the activation process with $ZnCl_2$ activation and its char without $ZnCl_2$ impregnation were compared. All samples showed higher distribution of mesopores surface area per unit mass, the mesopores were dissipated in the range of 2-5 nm diameter. Sopt had the maximum pore surface distribution of 1.76 cm^2/g at the pore width about 2.4 nm, while the others had their distribution trends rather be at micropores less than 2 nm.

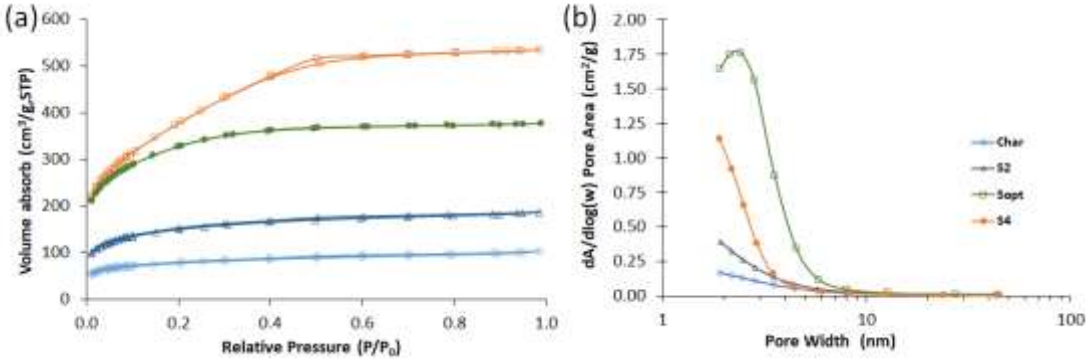

Figure 2 (a) N_2 adsorption/desorption isotherms and (b) pore size distribution

The morphologies of selected derived-AC and SCB-char were characterized as shown in Figure 3. Lignin was softened and removed from the bagasse surface during leaching with NaOH, the base leached-SCB structure presented scattering pores covering with some NaOH particles as seen in Figure 3(a). This chemical was eliminated from the char surface under heat treatment, so that carbonization of base leached-SCB at the optimum condition without $ZnCl_2$ activation caused the disruption of initial pores as revealed both micropores and mesopores distributed all over its surface (Figure 3(b)).The heat from carbonization can eliminate the chemicals like some volatile components blocked in the pores. Impregnation of SCB in $ZnCl_2$ prior to carbonization at the different condition gave more porous structure of activated carbons [7] as confirmed in Table 4 and Figure 2, S2 and Sopt presented the irregular pore shape with different pores size distribution as illustrated in Figure 3(c) and 4(d) respectively. As the effect of activating agent at the suitable carbonization condition, S4 had highest specific surface area owing mostly to mesopore structure which predominantly established on the outer surface while the micropores were located around the inner surface. At different resolutions of S4, the porous structure was distributed in the lateral side of AC surface (Figure 3(e)) and the different

sizes of pore individually dispersed with some interior smaller pores occurred along the pore transportation path (Figure 3(f)). S4 showed higher micropore proportion than the others resulted to higher nitrogen adsorption capacity and larger specific surface area as dicussed in the isotherm adsorption/desorption.

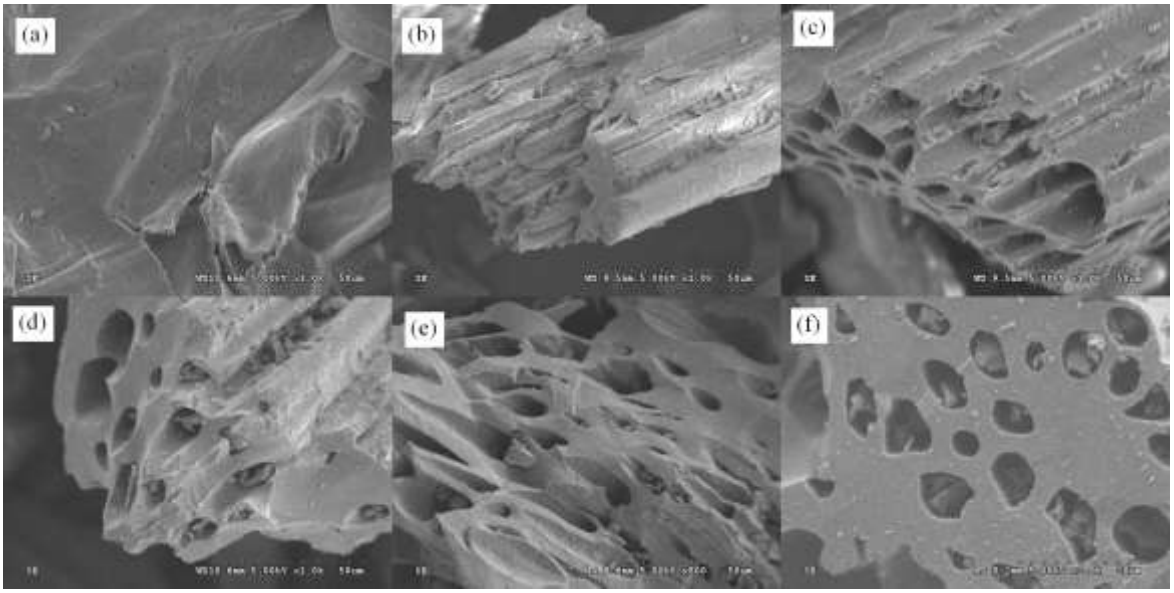

Figure 3 Scanning electron microscope images of : (a) base-leached SCB (x1k), (b) basec-leached SCB char ZnCl2 activation (x1k), , (c) S2(x1k) , (d) Sopt (x1k), (e) S4 (x0.8k) and (f) S4 (x2k)

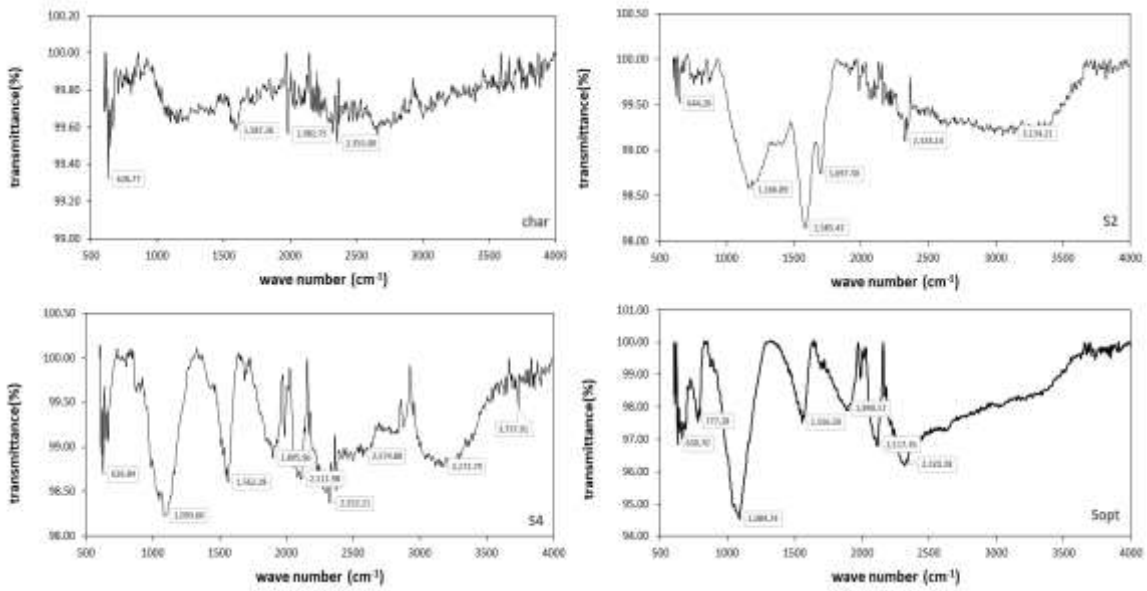

Figure 4 FTIR analysis of samples

The functional groups of SCB-char and AC surface were examined by the Fourier Transform Infrared Spectroscopy (FTIR, S5_iD5, Thermo Scientific Nicolet) recording in the IR spectrum range of 500-4000 1/cm. The different functional groups are characterized by the showing peaks at diverse wave numbers as shown in Figure 4. The FTIR spectrums of the obtained activated carbons were corresponded to the previous reviews [15]. The band around

630 1/cm and 646 1/cm were found in all samples indicating the represent of –C=C-H:C-H bend or alkenes functional group. The peak at around 779 1/cm was also found in S4 which has the largest specific surface area relative indicated aromatics. The longest peak presented in S4 and also S2 as the wide shallow one may be allocated to C–O stretch with the wave number between 920 1/cm and 1300 1/cm, and the peak at around 1089 1/cm may be belonging to structure of phenolic [15]. The presence of the C=O in the quinone structure were associated with the band wave number around 1589, 1554 and 1583 1/cm [15]. The band at around 1560 1/cm may be owing to an aromatic C-C ring stretching [16]. The band at around 1669 1/cm is related to the stretching of C=O as lactonic and carbonyl groups [15]. The band at around 2320 1/cm is the C-O bonds in ketone groups or the –COOH functional groups. A wide band located in the range of 3000-3500 1/cm is a consequence of phenolic O-H groups and adsorbed water [7].

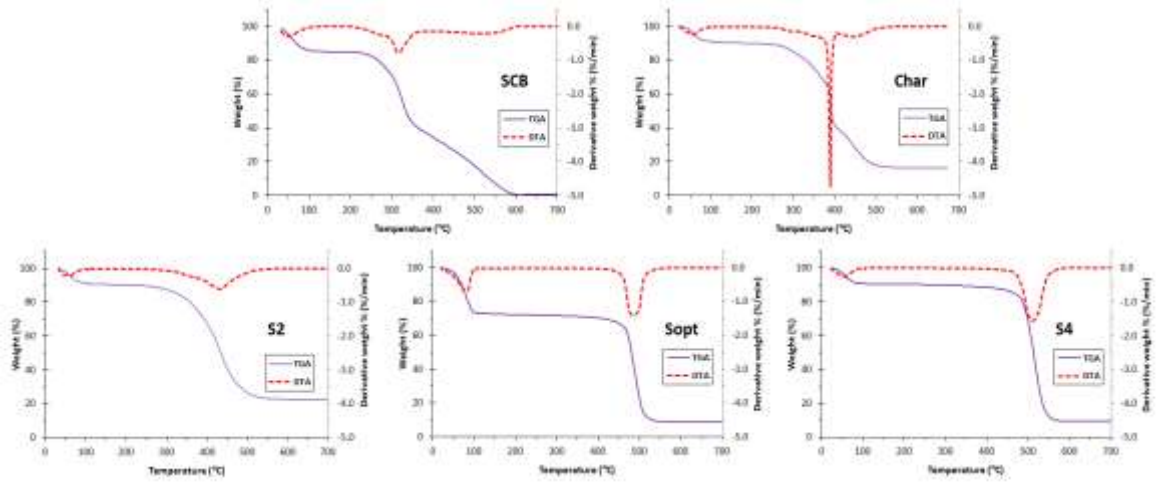

Figure 5 TGA and DTG thermograms for all selected samples.

Thermogravimetric analyzer (TGA, 50-Shimadzu Japan) was applied to analyze the thermal stability of selected samples by determining their mass losses as a function of temperature. For the base leached-SCB and SCB-char without chemical activation, three degradation stages were presented as seen in Figure 5. The weight losses in the region of temperature around 100-120°C was a first degradation in which water from the existence of moisture binding in water bonding form was evaporated called dehydration. The maximum weight loss rates of each sample were occurred at different tempertures in the second stage of temperature ranging from 180-400˚C. Due to the activating agent or $ZnCl_2$ as a natural Lewis acid in the AC with the impregnation of $ZnCl_2$, the dehydration process of carbon precursor could be raised by its nature lewis acid property as well as the volatile and tars was eliminated resulted from active pyrolysis occurred in this second stage at the temperature below 400˚C [5, 17]. The hemicellulose and cellulose also decomposed at this stage in the range of temperature of 180-270 and 270-400 respectively. The structure decomposition at the third stage starting at 400˚C to 550˚C indicates the material with high stability property [5]. These activated carbons showed the weight loss stage at the temperature range between 400-600˚C presenting volatization of $ZnCl_2$. These degradation behavaiors were similiar to the other publication related on $ZnCl_2$ activation in AC production [17]. It can been described as the active pyrolysis occurred along with reducing tar formation and carbon gasification of $ZnCl_2$. Especially in the peak at about 500˚C, the oxidation reactions were stimulated via catalyzing from the mechanism of

its own lewis acid property that supports the condensation reactions of aromatic which caused the increasing of aromatic content [17]. The fixed carbon as primitive structure was investigated above 550˚C. It can be seen that all activated carbons had higher amount of fixed carbon than precursor and unactivated char. Also, the last stage was belonged to the lignin decomposition which gradually took place from 200˚C to 900˚C. It had been concluded the primitive properties and final structure of activated carbons were dependent on several factors such as plant species, origin, weather conditions, quality and condition [5]. This study found that the produced activated carbons has high thermal stability comparable to the commercial activated carbon.

Conclusions

In this study, mesoporous structured SCB-AC with high specific surface area was produced via chemical impregnation-carbonization method. The predicted model with R^2 of 86.19% was obtained from ANOVA using Minitab 16 statistical software in experimental design.. The optimum condition was using 2.19 M of $ZnCl_2$ for SCB impregnation followed by carbonization at 488.89˚C for 95.18 min was 1,298 m^2/g. This prediction model was reliable with only 1.07% error. The SCB-AC consisting of micro- and- meso- irregular pores with maximum specific surface area of 1,355.7 m^2/g was achieved from using $ZnCl_2$ concentration of 2 M and carbonization at 500˚C for 90 min. Carbonization exceeded than 500 ˚C resulted to the reduction of AC specific surface area. This study revealed that $ZnCl_2$ concentration had stronger effect on the porous characteristics than the other factors; carbonization temperature and activation time. The produced AC composed of similar functional groups to other previous work and had high thermal stability .

Acknowledgements

The project was supported by Centre for Alternative Energy Research and Development (AERD), Khon Kaen University, THAILAND.

References

1. Danish M, Ahmad T. A review on utilization of wood biomass as a sustainable precursor for activated carbon production and application. Renew Sustain Energy Rev. 2018; 87: 1–21.
2. Elmouwahidi A, Bailón-García E, Pérez-Cadenas AF, Maldonado-Hódar FJ, Carrasco-Marín F. Activated carbons from KOH and H_3PO_4-activation of olive residues and its application as supercapacitor electrodes. Electrochim Acta. 2017; 229: 219–228.
3. Viswanathan B, Neel P, Varadarajan T. Methods of activation and specific applications of carbon materials. Methods Act Specif Appl Carbon Mater. 2009; 160.
4. Pagketanang T, Artnaseaw A, Wongwicha P, Thabuot M. Microporous activated carbon from KOH-activation of rubber Seed-shells for application in capacitor electrode. Vol. 79, Energy Procedia. Elsevier B.V.; 2015: 651-656.
5. González-García P. Activated carbon from lignocellulosics precursors: A review of the synthesis methods, characterization techniques and applications. Renew Sustain Energy Rev. 2018; 82: 1393–1414.

6. Bachrun S, Ayurizka N, Annisa S, Arif H. Preparation and characterization of activated carbon from sugarcane bagasse by physical activation with CO_2 gas. IOP Conf Ser Mater Sci Eng. 2016; 105(1).
7. Liou TH. Development of mesoporous structure and high adsorption capacity of biomass-based activated carbon by phosphoric acid and zinc chloride activation. Chem Eng J. 2010; 158(2): 129–142.
8. Sulaiman NS, Hashim R, Mohamad Amini MH, Danish M, Sulaiman O. Optimization of activated carbon preparation from cassava stem using response surface methodology on surface area and yield. J Clean Prod. 2018; 198: 1422–1430.
9. Nurul-Shuhada Md-Desa, Zaidi Ab Ghani, Suhaimi Abdul-Talib, Chia-Chay Tay. Optimization of activated carbon preparation from spent mushroom farming waste(SMFW) via box-behnken design (Penyediaan Secara Optimum Arang Teraktif daripada Sisa Tanaman Cendawan Terpakai. Malaysian J Anal Sci. 2016; 20(3): 461–468.
10. Das S, Mishra S. Box-Behnken statistical design to optimize preparation of activated carbon from Limonia acidissima shell with desirability approach. J Environ Chem Eng. 2017; 5(1): 588–600.
11. Saka C, BET, TG-DTG, FT-IR, SEM. iodine number analysis and preparation of activated carbon from acorn shell by chemical activation with $ZnCl_2$. J Anal Appl Pyrolysis. 2012; 95: 21–24.
12. Hu Z, Srinivasan MP, Ni Y. Preparation of mesoporous high-surface-area activated carbon. Adv Mater. 2000; 12(1): 62–65.
13. Zhu Z, Li A, Yan L, Liu F, Zhang Q. Preparation and characterization of highly mesoporous spherical activated carbons from divinylbenzene-derived polymer by $ZnCl_2$ activation. J Colloid Interface Sci. 2007; 316(2): 628–634.
14. Demiral H, Demiral, Karabacakoglu B, Tümsek F. Adsorption of textile dye onto activated carbon prepared from industrial waste by $ZnCl_2$ activation. J Int Environ Appl Sci. 2008; 3(5): 381–389.
15. Tsai WT, Chang CY, Lin MC, Chien SF, Sun HF, Hsieh MF. Adsorption of acid dye onto activated carbons prepared from agricultural waste bagasse by $ZnCl_2$ activation. Chemosphere. 2001; 45(1): 51–58.
16. Tran VT, Quynh BTP, Phung TK, Ha GN, Nguyen T, Bach LG, et al. Production of activated carbon from sugarcane bagasse by chemical activation with $ZnCl_2$: Preparation and characterization study. Res J Chem Sci. 2016; 6(5): 42–47.
17. Tsai WT, Chang CY, Lee SL, Wang SY. Thermogravimetric analysis of corn cob impregnated with zinc chloride for preparation of activated carbon. J Therm Anal Calorim. 2001; 63(2): 351–357.